

Microscopic modelling of ignition and burning for well-arranged energetic crystals in response to drop-weight impact

Yanqing Wu¹ Fenglei Huang¹ Min Zhou²

¹ State key Laboratory of Explosion Science and Technology, Beijing Institute of Technology, 100081, Beijing, P. R. China

² The George W. Woodruff School of Mechanical Engineering, Georgia Institute of Technology, Atlanta, Georgia 30332-0405, USA

E-mail: wuyqing@bit.edu.cn (Yanqing Wu)

Abstract. To probe into impact sensitivity of energetic crystals, a theoretical approach was developed for modelling a single layer of energetic particles between upper striker and below base. Considering the particle plasticity, frictional heating, melting, fracture, and chemical reaction at particle level, effects of loading parameters and sample characteristics on time-to-ignition and burning rate were compared. Finite element numerical simulations were simultaneously performed to provide supporting evidence for thermo-mechanical interactions among energetic particles. Once hot-spots ignition occurred during impact, the macrokinetics of chemical reactions were formulated by hot-spots density, combustion wave velocity and geometric factor. The resulting reaction may or may not develop into a violent event, may be sustained or be extinguished, which can be revealed from the subsequent burn reaction rate.

1. Introduction

It has long been necessary to postulate the existence of an energy localization process in order to explain the sensitivity of explosives to low-level impact. The drop-weight test is the simplest and most commonly used method of assessing the sensitivity of low-velocity impacted explosives [1,2]. However, drop weight test sensitivity data from various laboratories usually are not consistent with each other. Most sensitivity evaluation tests focus on experimental determinations of ‘go/no go’ conditions [3,4], with limited efforts toward identifying the underlying ignition micro-mechanisms.

There are many possible hot spot sources at nano- or microscopic scale, including dislocations, voids, twins, inclusions. However, when dropping a hammer onto a granular explosive charge, contacts with other particles or with the solid walls at mesoscopic scale play the key role for temperature fluctuation or deformation localization at engineering scale. Friedman correlated thermal explosion with the impact sensitivities of several explosives [5]. Francis and Cuthbert used finite element analysis of the drop-weight test to calculate the temperature in the localized zones near the sample periphery [6]. In the drop-weight system, ignition mechanisms such as adiabatic shear bands, trapped gas spaces, viscous flow, friction, fracture and triboluminescent discharge have ever been discussed [7].

The present model was established by working out kinematic equations for a layer of well-arranged impacted HMX particles, considering frictional heating, micro-impact plasticity and breakage of particles. It is capable of describing the following events: 1) how the drop weight mechanical energy will be transferred to the sample, 2) what kind of localized energy that is focused in



local regions upon impact, 3) whether or not the reaction developed from these hot spots into a violent burning.

2. Finite element model

The finite element simulations were performed based on commercial software code ABAQUS/Explicit. Axisymmetric displacement boundary conditions were imposed on a quarter of the cylindrical striker, base anvil and target explosive charge, as shown in figure 1. All outside surfaces remained to be ambient temperature (300K). Current simulation used simple thermal elastic-plastic constitutive equations for the energetic crystals [8] and elastic responses for striker and base. There existed friction heating, plastic dissipation energy and heat conduction between neighbour particles, and between particles with impacting contact surfaces.

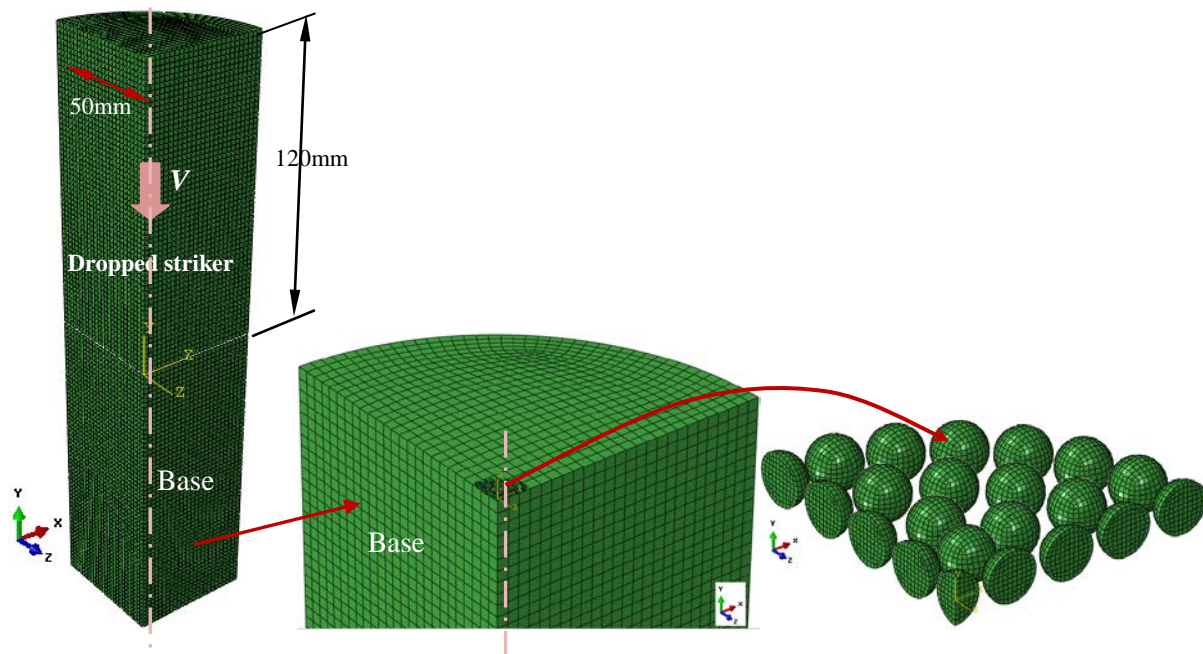


Figure 1 Simplified finite element model for analyzing thermal-mechanical process of energetic grains in response to the drop-weight impact loading.

2.1. Simulated pressure curves and distributed area evolutions

Figure 2(a) presented the evolution of average pressure applied to the explosive charge subjected to 10.0, 15.0, 20.0cm drop height impact and 7.36kg drop weight. The maximum average pressures are 206.2, 386.3, and 546.8 MPa for the 10.0, 15.0 and 20.0cm drop height impact, respectively. Each impact process undergoes the loading and unloading stage. With the drop height increased, the duration of the process decreased and the maximum average pressure increased.

Thickness evolution of the single layer of explosive charge was presented in figure 2(b). The explosive charge can be compressed from original thickness (1.0mm) to the lowest value 0.43, 0.38 and 0.35mm for the 10.0, 15.0 and 20.0cm drop height, respectively. The thickness decreased monotonously till the pressure decreased to zero. Once the pressure became zero, the thickness began to bounce to some extent as the result of elastic recovery.

Figure 2(c) showed the kinetic energy and plastic dissipation energy during the period of impact, from which the fraction of kinetic energy f_{eff} absorbed by the sample can be calculated. The value f_{eff} were 0.88, 0.77, 0.69 for 10, 15 and 20cm drop height impact, respectively.

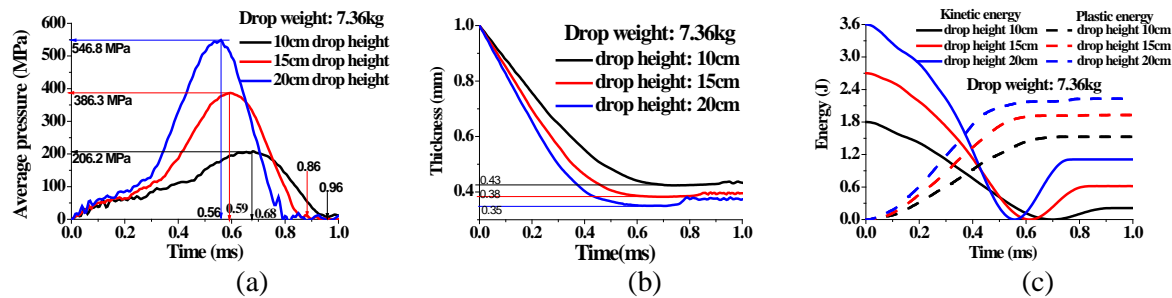


Figure 2 Comparisons for Simulated (a) average pressure evolution; (b) thickness of the explosive charge; (c) kinetic energy and plastic dissipation energy.

2.2. Simulated temperature distributions and heat flux

Figure 3 presented the pressure contours for the energetic grains subjected to 20cm drop-weight impact. Pressure localization can be observed at the contact surfaces for each particle at 250 μ s, as well as in the centre of the charge with large-scale linkages were formed till 500 μ s. The degree of pressure concentration in the centre was more serious at time 700 μ s than at 500 μ s. There appeared tensile pressure regions along the boundary of explosive charge with the development of impact process, as shown in figure 5(b) and (c).

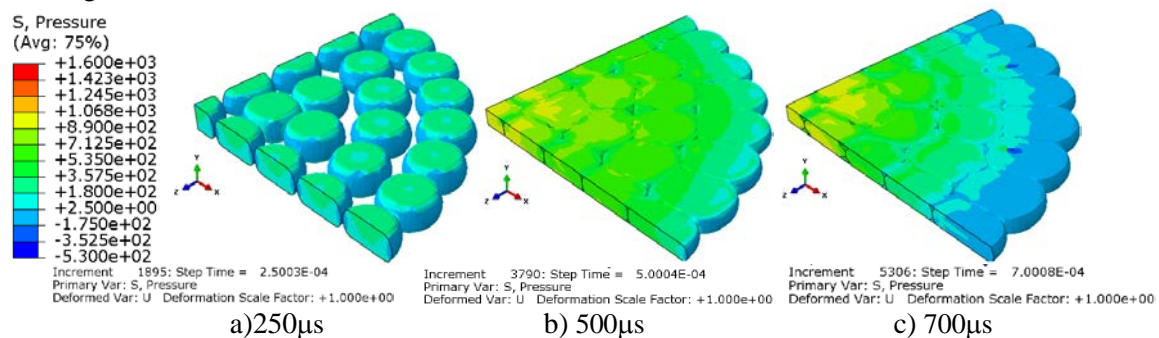


Figure 3 Simulated pressure distributions over the energetic grains at different moment subjected to 7.36 kg drop-weight and 20 cm drop height.

Figure 4 showed the heat flux leaving each particle surface per unit area through three different paths: grains interface; upper impact surface and below anvil surface. Once the impact began, the upper dropped surface took away heat from particle's surface (at about 0.04ms). Subsequently, with the stress wave propagated, heat flux leaving the grains from below surface needed to be taken into account (at about 0.11ms). When grains deformed to contact with each other, heat flux leaving grain's interface performed a key role (at about 0.3ms). Heat flux in figure 4 implied that heat conduction can be formulated based on one-dimensional system at early stage and then should be transformed to cylindrical-coordinate system for later stage.

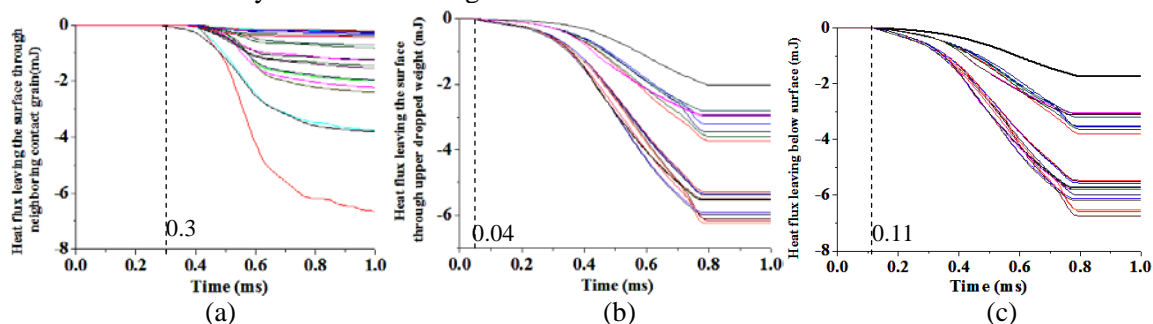


Figure 4 Heat flux leaving per unit area surface of each particle through a) neighbour grains; b) upper impacted surface; c) below anvil surfaces.

3. Theoretical model

3.1. Mechanics analysis

Based on numerical simulated results, the explosive charge composing of well-arranged energetic crystals without overlaps impacted by the upper dropping striker was modelled. Figure5 (a) explained the approach for modelling a single layer of separate crystals between striker and base. Figure5(b) provides an illustrative graph of contact mechanics for an individual particle prior to fragmentation. To simplify the calculations, energetic crystals were assumed be equal-sized spherical particles with initial diameter d_0 (mm) and spacing of w_0 (mm). The explosive charge occupied an initial circular area with diameter d_{s0} (mm).

The motion of the dropped striker during impact was determined from its momentum balance,

$$\ddot{x}_u = g - \frac{F_c(t)}{M_w} \quad (1)$$

where x_u denoted the falling distance of the striker, g is the acceleration of gravity, and $F_c(t)$ is the force applied to the explosive charge by the weight. A simple relationship between the energy absorbed by sample (W_{sample}) and the input kinetic energy (W_{inp}) was used,

$$W_{sample} = f_{eff}(H_0)M_w g H_0 \quad \text{or} \quad \dot{W}_{sample} = f_{eff} \cdot \dot{W}_{inp} = M_w \dot{x}_u \ddot{x}_u \quad (2)$$

Dependence of coefficient f_{eff} on initial drop height H_0 can be obtained based on the numerical results. More detailed formulas can refer to the literature [9,10].

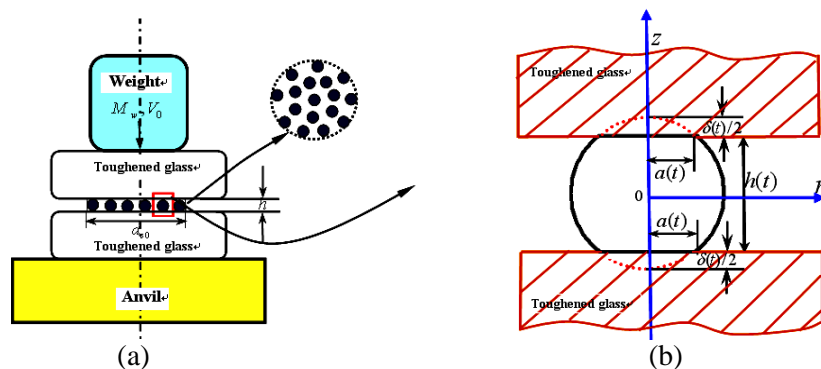


Figure 5 Schematic graphs explaining the drop-weight impact process with (a) global drop-weight model, (b) contact deformation of individual particle.

3.2. Thermal analysis

In the course of an impact event, heat generation by friction, irreversible plastic work, and chemical reaction heat, as well as heat conduction through the contact surface, determined the flash temperature rise at those hot spots. Prior to ignition, each particle was regarded as the separated and linked heat sources at different stages as shown in figure 6(a).

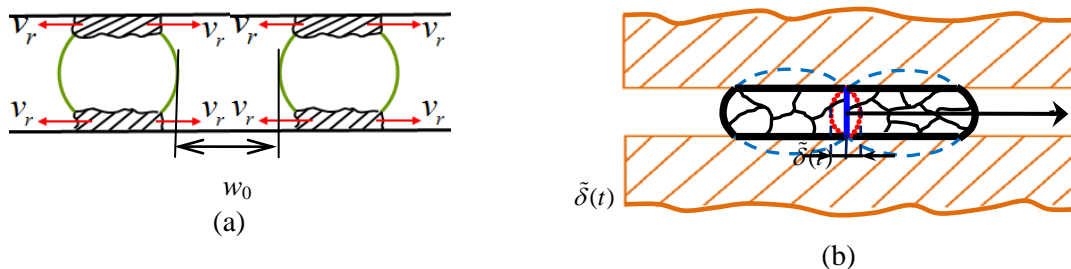


Figure 6 Thermal model for analyzing ignition and hot spots growth to burning a) separated heat source before ignition; b) linked heat source when severe deformation occurs.

As a function of r , z , and t , equation of conduction reduced to,

$$\frac{\partial T}{\partial t} = \kappa_s \left(\frac{\partial^2 T}{\partial r^2} + \frac{1}{r} \frac{\partial T}{\partial r} + \frac{\partial^2 T}{\partial z^2} \right) + \frac{\dot{Q}(t)}{m_p C_v} \quad 0 \leq r < a(t) \quad (3)$$

where $\dot{Q}(t) = \dot{w}_{chem} + \dot{w}_{plast} + \dot{w}_{frict} - \dot{q}_{melt}$, \dot{w}_{chem} , \dot{w}_{plast} , \dot{w}_{frict} were chemical heat, plastic dissipated energy and frictional heat per unit time, respectively. m_p , κ_s and C_v were the particle mass, thermal Diffusivity and specific heat of HMX material.

$$\dot{W}_{sample} = \dot{W}_{plast} + \dot{W}_{frict} + \dot{W}_{surf} = f_{eff} \cdot \dot{W}_{inp} \quad (4)$$

For a reactive material, temperature rise was the result of the sum of chemical heat and mechanical dissipation. Arrhenius chemical reaction rate was employed,

$$\dot{w}_{chem} = q_r Z_r \exp(-E_A / R_g T) \quad (5)$$

where q_r was the heat of chemical decomposition per unit mass and $Z_r e^{-E_A / RT}$ was the Arrhenius expression of the reaction rate. Initial and boundary conditions were slightly dependent of the coordinate value θ in cylinder system at least prior to breakage.

$$T = T_0 \quad (0 < r < a(t), \quad t = 0) \quad (6)$$

$$\kappa_s \left(\frac{\partial^2 T}{\partial r^2} + \frac{1}{r} \frac{\partial T}{\partial r} \right) + \frac{\dot{Q}(t)}{m_p C_v} \quad (z = h(t)/2 \quad \text{and} \quad z = -h(t)/2) \quad (7)$$

$$\frac{\partial T}{\partial t} = \kappa_s \frac{\partial^2 T}{\partial z^2} \quad (z > h(t)/2 \quad \text{and} \quad z < -h(t)/2) \quad (8)$$

Following the interpretation of the concept of hot spots proposed by Lobanov [11], the macrokinetic reaction velocity $d\lambda / dt$ can be formulated as a product of three terms [12],

$$d\lambda / dt = \alpha M^{1/3} \cdot D_c \cdot F(\lambda) \quad (9)$$

where α , M , D_c were the constant, density of ignited hot spots, the propagation velocity of the combustion wave, respectively. The geometric factor F was introduced to take into account the change in combustion topology.

3.3. Results analysis

Figure 7(a) presented times-to-ignition vs. frictional coefficients between HMX and impact surface subjected to different drop-height impacts, keeping other conditions the same. It showed that time-to-ignition decreased with the increase of frictional coefficients. Each curve provided a threshold value of frictional coefficients, below which ignition never occurred. A careful examination demonstrated that ignition occurred later with freshly polished surfaces than rougher surfaces [13].

In figure 7(b), a series of calculations were conducted by altering Young's modulus of anvil materials. Time-to-ignition decreased with the increase of Young's modulus. Calculated results showed that harder anvil material leads to shorter loading time and promotes the ignition process.

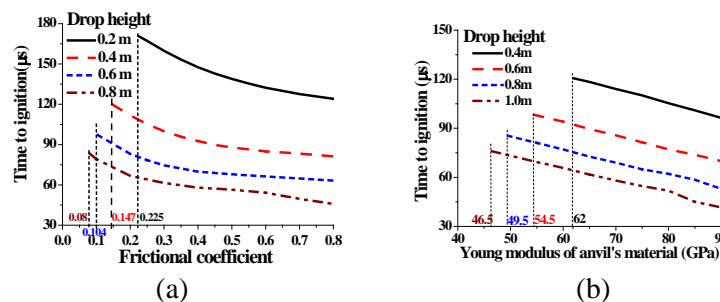


Figure 7 Dependence of time-to-ignition on (a) frictional coefficients between explosive and contact surfaces; (b) Young's modulus of the below anvil material.

Figure 8 provided the effects of drop heights, drop weights and porosity on the macroscopic burn reaction rate evolutions. The burning reaction rate showed that the heavier the drop weight was, the more intense the burn chemical reaction was. Different loose degree distribution of grains influenced both macroscopic burn reaction beginning time and its violence.

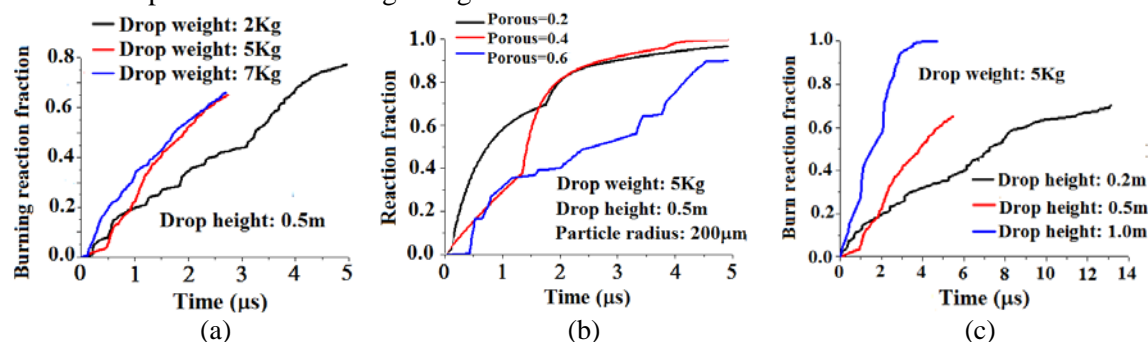


Figure 8 Predictions of the burning reaction rate on various (a) drop weights; (b) porosity; and (c) drop heights.

4. Conclusions

It has long been necessary to postulate the existence of an energy localization process in order to explain the sensitivity of explosives subjected to low-level impact. Numerical simulated results provided the heat flux and mechanical interactions among particles, and particles and contact surface. The results supported our assumptions proposed for subsequent theoretical model. Based on assumptions including given absorbed energy, equal-sized spherical particles, one-dimensional wave propagation, a micromechanics theoretical approach was developed to calculate hot spots formation and growth to burning for a single layer of impacted energetic particles. Threshold frictional coefficients and Young's modulus of anvil material for ignition to occur can be calculated for the HMX granular explosives. The calculated results implied that simple ordering of sensitivity for explosive materials based on drop weight impact experiments is very difficult.

Acknowledgments

The authors are very grateful for the reviewer's instructive suggestions and careful proofreading, and would like to acknowledge the National Natural Science Foundation of China (Grant No. 11172044).

References

- [1] Balzer J E, Proud W G, Walley S M and Field J E 2003 *Combust. Flame.* **135** 547
- [2] Balzer J E, et al. S M 2002 *Combust. Flame.* **130** 298
- [3] Baker P J and Mellor A M 1997 *Combust. Sci. Technol.* (Book Ser.) **4** 289.
- [4] McNesby K L and Coffey C S 1997 *J. Phys. Chem. B.* **101** 3097.
- [5] Friedman M H 1963. *9th Symposium International on Combustion* (Academic Press;New York) p 294
- [6] Francis E C and Cuthbert B M 1987. *JANNAF Propulsion Systems Hazards Subcommittee Meeting* vol 1 (CPIA Publication) p257
- [7] Field J E, et al. 1992 *Phil. Trans. Math. Phys. Eng. Sci.* **339** 269
- [8] Bonnett D L and Butler P B 1996. *J. Propul. Power.* **12** 680
- [9] Johnson K L 1985 *Contact Mechanics* (Cambridge University Press, New York) p 93
- [10] Wu Y Q, Huang F L and Huang M 2012 *Propell. Explos. Pyrotech.* **38** 214
- [11] Lobanov V F 1980 *Fiz. Goreniya Vzryva* **16** 113
- [12] Grebenkin K F, et al. S 2006 *Combust. Explo. Shock Waves* **42** 598
- [13] Coffey C S and DeVost V F 1995 *Propell. Explos. Pyrotech.* **20** 105